Available online at www.sciencedirect.com

ScienceDirect

Procedia Engineering 147 (2016) 854 – 859

Procedia Engineering

www.elsevier.com/locate/procedia

11th conference of the International Sports Engineering Association, ISEA 2016

A 3D numerical model for the optimization of running tracks performance

L. Andena[a,c], S. Aleo[a], F. Caimmi[a], S. Mariani[b,c], F. Briatico-Vangosa[a] and A. Pavan[a]

[a]*Dipartimento di Chimica, Materiali e Ingegneria Chimica, Politecnico di Milano, Piazza Leonardo da Vinci 32, 20133, Milano, Italy*
[b]*Dipartimento di Ingegneria Civile e Ambientale, Politecnico di Milano, Piazza Leonardo da Vinci 32, 20133, Milano, Italy*
[c]*E4Sport - Engineering for Sport Laboratory, Politecnico di Milano, Piazza Leonardo da Vinci 32, 20133 Milano, Italy*

Abstract

In previous works, a finite element model of the shock absorbing characteristics of athletics tracks was developed, able to give sufficiently reliable predictions from laboratory tests performed on suitable material samples. The model proved to be effective in discriminating the effects of geometry (i.e. thickness) and material properties (essentially the elastic characteristics) on force reduction, thus allowing a first optimization of the tracks in view of their approval by the International Association of Athletics Federations (IAAF).
This simplified 2D model neglected the real track structure, considering it as a single layer of material having homogenized properties. In the present study, a new 3D model was developed to accurately describe the structure of multi-layered tracks, with properties and geometrical construction (e.g. solid or honeycomb) differing from one layer to another.
Several tracks having different combinations of top/bottom layers varying in both material formulation (i.e. chemical composition) and geometry were thus considered. Mechanical properties of the individual elements constituting the track were measured with small-scale laboratory tests, taking into account their strain-rate dependence.
The 3D model allowed a complete representation of the loads acting on the track and it gave results which are in very good agreement with the experiments. This proves it to be a valuable tool for the purpose of optimizing the track in terms of material formulation as well as layer geometrical construction and arrangement: as an example, the effect of changing the cell size of the honeycomb pattern was investigated.

Peer-review under responsibility of the organizing committee of ISEA 2016

Keywords: athletics tracks; modeling; mechanical properties; geometry optimization

1. Introduction

Athletics tracks house many different competitions including running, jumping and throwing events. Although each specialty envisages different athletics gestures, these surfaces are designed to reach the best compromise between the different necessities of the athletes expected to exploit them, most notably including safety and performance. Nowadays rubbery synthetic tracks substituted both grass tracks and later mineral porous surfaces nearly all over the world, thanks to their better dynamic properties and lower maintenance needs.

The International Association of Athletics Federations (IAAF) recognises the shock absorption ability of an athletics track as having a pivotal role to ensure the athletes' safety and comfort. The main parameter employed to describe the impact behaviour of a surface is called force reduction (*FR*), defined according to:

$$FR = \left(1 - \frac{F_t}{F_r}\right) \cdot 100 \quad (1)$$

where F_t represents the impact peak force measured on a track whereas F_r is the reference value of peak force, obtained on the pavement foundation. Such measurements are carried out with the Artificial Athlete Berlin (sketched in Fig. 2(a)) according to standard EN 14808 [1], and tracks must exhibit a *FR* value between 35% and 50% to be approved by IAAF. Previous studies [2]

* Corresponding author. Tel.: +390223993289; fax: +390223993280.
E-mail address: luca.andena@polimi.it

Peer-review under responsibility of the organizing committee of ISEA 2016
doi:10.1016/j.proeng.2016.06.291

demonstrated that the *FR* parameter depends on both the pavement thickness and the material properties, mainly in terms of the elastic response.

A simplified two-dimensional (2D), axisymmetric finite element (FE) numerical model was implemented in earlier works [3-4], representing the impact of the Artificial Athlete Berlin on different tracks. Its reliability was assessed by comparing numerical predictions with the results of laboratory tests performed on suitable material samples. Such a model neglected the real track structure, considering it as a single layer of material having homogenized properties. On the contrary, pavements used in international competitions are usually composed by two layers having different mechanical properties and structure: a coloured top finishing layer, possessing good wear resistance, and a bottom base layer, which is mainly responsible for the shock absorbing characteristics of the track. In particular, a honeycomb design with different shapes (e.g. rectangular or hexagonal) is often produced on the base layer by calendering.

The scientific literature offers some examples [5-6] of very simple three-dimensional (3D) FE models of sports surfaces; in the present study, a new one was developed to accurately describe the structure of such multi-layered tracks and, consequently, allow an optimization of the track impact performance, which is not limited to the vertical direction.

2. Experimental methods

Three pavements were considered in this work, differing in terms of the honeycomb geometry of the base (see Fig. 1) and composition of one or both layers; they were all produced by Mondo S.p.A., the Olympic Games official supplier. In this study each layer is considered as a separate material (see Table 1).

In order to characterize the materials from a mechanical point of view, quasi-static uniaxial compression experiments were performed using a screw-driven Instron 1185R5800 dynamometer on square specimens (30 mm side) cut from each track. The finishing and base layers of each track were also similarly tested. Compression tests were run up to stretches of 0.6 (stretch being the ratio between current and initial height of the sample). According to previous works [4], after an impact with the Artificial Athlete Berlin the track deforms with a stretch rate of about 60 s^{-1}, which is unattainable with quasi-static testing. Therefore, tests at different stretch rates (0.006 s^{-1}, 0.06 s^{-1} and 0.6 s^{-1}) were performed and the desired data curve at 60 s^{-1} was obtained by linearly extrapolating stress vs. log(rate) data for each level of stretch, in 0.01 intervals. Given the good repeatability of the experimental results, only three tests were carried out per material and stretch rate. Data at 60 s^{-1} was then fitted with suitable material models to be used within the numerical simulations.

In parallel with tests on material samples, *FR* tests were performed; five dropping events were carried out and a very good repeatability was observed in the resulting force vs. time curves. In order to compare them with the FE model predictions, both experimental and numerical data were processed with a low-pass, ninth order Butterworth filter with cut-off frequency of 120 Hz, as required by IAAF standards.

Table 1. Materials considered in the present work, and legend of the related labels. Note: tracks C and F slightly differ in terms of both composing material and dimensions of the hexagonal base layer structure.

Complete track	Finishing layer	Base layer
A Mondotrack 1	B Mondotrack 1	C hexagonal 1
D Mondotrack 2	E Mondotrack 2	F hexagonal 2
H Mondotrack 3	I Mondotrack 3	L rectangular

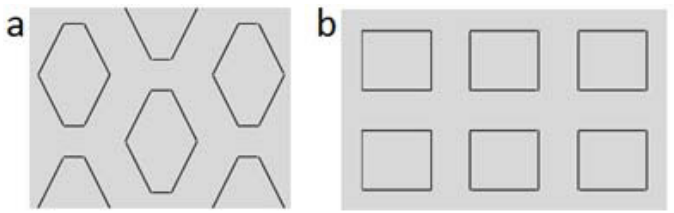

Fig. 1. Qualitative sketch of the base layer structures of tracks (a) C and F, and (b) L.

3. Numerical modelling

3.1. Constitutive equations

In most cases the Mooney-Rivlin hyperelastic model proved able to represent in an accurate way the material behaviour. For the incompressible case, the stored energy U can be written in terms of the principal invariants I_1 and I_2 of the left Cauchy-Green strain tensor, as:

$$U = C_{10} \cdot (I_1 - 3) + C_{01} \cdot (I_2 - 3) \tag{2}$$

where parameters C_{10} and C_{01} were chosen to best fit each material curve at 60 s^{-1}.

The compressive behavior of the separate finishing layers (materials B, E and I) turned out instead to be better represented by an incompressible two-term Ogden hyperelastic model, with a stored energy given by:

$$U = \sum_{i=1}^{2} \frac{2\mu_i}{\alpha_i^2} \left(\lambda_1^{\alpha_i} + \lambda_2^{\alpha_i} + \lambda_3^{\alpha_i} - 3\right) \tag{3}$$

where λ_1, λ_2, and λ_3, are the principal stretches, and parameters μ_i and α_i were set for each material again to best fit the experimental data. Finally, material F was fitted using a single-term Ogden model.

3.2. Quasi-static compression test

With the previous 2D model, overall equivalent homogenized material properties for the whole track were obtained from the experiments, see [4]. To tune the constitutive parameters under a uniaxial stress state, the stretch field was assumed uniform in the specimen and data were best fitted (through least-squares) with an analytical solution.

The 3D model here adopted requires instead a definition of the intrinsic properties of each constituent material, including that of the honeycomb structure; for the latter, it is very difficult to extract samples suitable for the evaluation of material properties. Hence, a detailed FE model was developed for the compression tests, using the general-purpose commercial code Abaqus [7]. The specimens were modelled explicitly accounting for the geometry of the base layer, so as to catch the finite-strain evolution of sample geometry and compliance under the external loading. The relative vertical displacement of the top and bottom surfaces of the specimen was imposed according to the displacement of the loading plates, as recorded during the compression test. The specimens were space-discretized with four-node tetrahedral elements with a hybrid formulation. The layer response (extrapolated up to stretch rates of 60 s^{-1}) in terms of vertical load vs. displacement, or equivalently nominal stress vs. stretch, was best fitted using the constitutive models mentioned in Section 3.1.

3.3. FR test

During the *FR* test, see Fig. 2, a dropping mass of 20 kg strikes, at 1 m/s, the upper surface of a spring, laying on the load cell. The load cell, in turn, transfers the impact load on the test foot, a cylinder with rounded edges weighing 0.651 kg which represents the athlete's heel, resting on the track to be tested. Finally, the track is supported by a concrete substrate.

The steel parts of the system (mass, spring, load cell and test foot) were modelled as either rigid or isotropic elastic bodies, with a Young's modulus E_s =200 GPa and a Poisson's ratio ν_s =0.3. The concrete foundation on which the track rests was modelled as an isotropic elastic body too, with a Young's modulus E_c =30 GPa and a Poisson's ratio ν_c =0.15. The spring and the load cell were instead modelled as couples of thin plates connected through springs, respectively featuring an axial stiffness of 2 MN/m and 1 GN/m, and a mass of 1.46 kg and 0.518 kg.

To compare the results of this model with those of the previous 2D one, the track was first modelled as a homogeneous hyperelastic body. Next, the actual geometry of each layer was considered, with the top and bottom one perfectly bonded to each other. Individual layers were described with the hyperelastic constitutive models mentioned in Section 3.1, all tuned according to the procedure detailed in Section 3.2. The 3D geometry of the base layers was introduced to correctly account for the local stress state within the honeycomb structure. Allowing for the two-fold symmetry of geometry and loading condition, only one quarter of the test rig was modelled and discretized in Abaqus. The contact between surfaces of the bodies interacting during the test was handled as a "hard" type (allowing no overclosure between the opposing surfaces). The layers were discretized using eight-node hexahedral elements with reduced integration and a hybrid formulation; such elements are somehow tailored for the volume-preserving hyperelastic materials under study. The mesh density for the whole track was accurately selected to assure the results to be mesh-independent and to avoid spurious oscillations in the load evolution measured by the spring representing the load cell.

To assess the influence of the base layer honeycomb geometry on the vertical impact response of the considered tracks, the characteristics of such structure were modified, and numerical simulations were run to investigate the resulting behaviour of the flooring. The finishing layer characteristics were kept unchanged, as well as the base layer's thickness and the depth of its cells,

whereas in-plane cell dimensions were modified to scale. In particular, the following variations were considered with respect to the original structure: -40%, -20%, +20%, +40% and +80%. Only tracks A and H were considered in this phase, due to the similarity between the base layer geometries of tracks A and D.

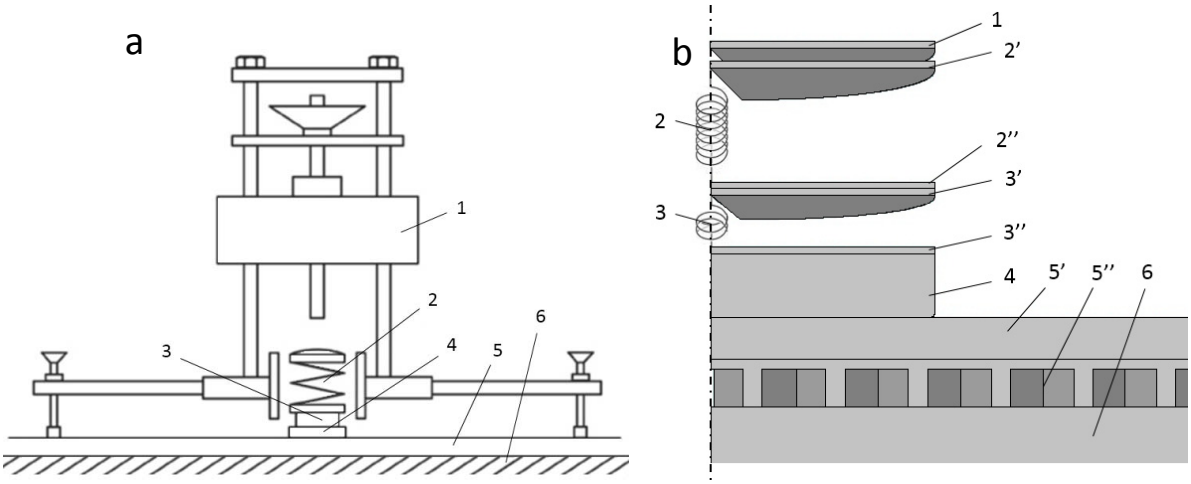

Fig. 2. (a) Sketch of the Artificial Athlete Berlin, and (b) adopted numerical model. *1* Dropping mass, *2* spring (*2'* upper and *2''* lower plates), *3* load cell (*3'* upper and *3''* lower plates), *4* test foot, *5* track (material A, in the specific case, composed by *5'* finishing and *5''* base layers; darker areas represent the structure voids), *6* substrate.

4. Results and Discussion

Fig. 3 (a) shows the experimental compression stress-stretch curves obtained for material A along with the extrapolation at a stretch rate of 60 s^{-1}; extrapolated results for all the materials are presented in Fig. 3 (b). The values of the material parameters that were employed in the numerical model for each material are listed in Table 2. For the base layer materials two sets of parameters are given: the first one corresponds to the fitting done directly on the compression test results, i.e. assuming that the structured layer behaves as an equivalent homogenous solid; the other set (labelled *3D*) comes from the compression test modelling described in section 3.2 and represent the actual behavior of the bulk material.

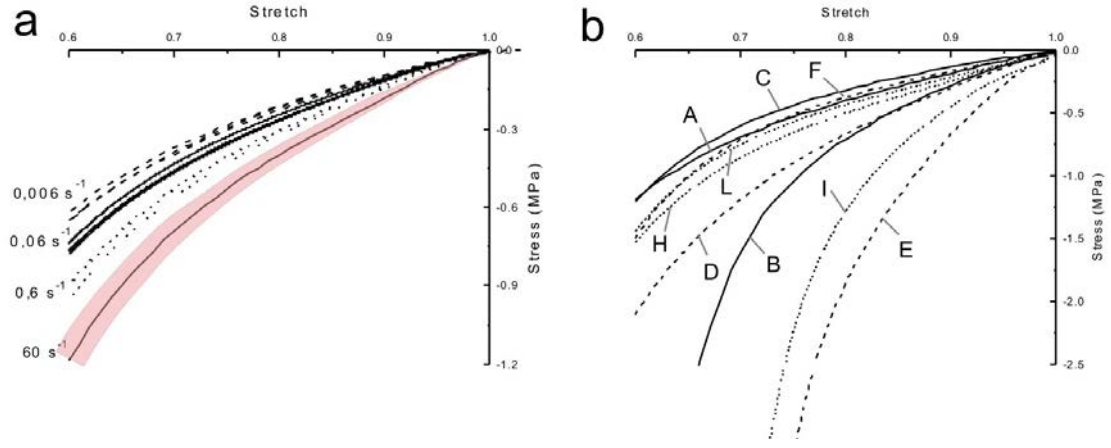

Fig. 3. (a) Stress-stretch curves obtained from the compression tests on material A at different stretch rates; (b) Compression behavior expected from all the materials at a stretch rate of 60 s^{-1}. The shaded area in Fig. 3 (a) represents the standard deviation related to the fitting performed.

Table 2. Constitutive parameters used for the materials under study, as obtained from the best fit of compression data. 3D entries represent the parameter sets identified by hand-fitting data from the 3D simulations including the actual honeycomb structure of the three base layers (C-F-L).

Material	Mooney-Rivlin model		Ogden model			
	C_{10} (MPa)	C_{01} (MPa)	μ_1 (MPa)	α_1	μ_2 (MPa)	α_2
A	0.23	0.02				
B			1.03	8.90	0.00	-18.21
C	0.000	0.16				
C (3D)	*0.12*	*0.16*				
D	0.30	0.10				
E			2.25	12.21	0.02	-20.88
F			0.54	6.36	-	-
F (3D)	*0.06*	*0.22*				
H	0.27	0.04				
I			1.76	10.14	0.01	-21.51
L	0.16	0.09				
L (3D)	*0.38*	*0.07*				

Considering now the FR test, Fig. 4 shows the trend in the force exchanged between the test foot and the tracks with the elapsing impact time, processed as previously noted with a ninth order Butterworth filter with a cutoff frequency of 120 Hz. For each material, the curves resulting from the Artificial Athlete Berlin tests and from the related 3D simulations are compared; simulations include both the homogenized model and the one which includes the actual base layer geometry. All the relevant values of FR are listed in Table 3, together with the percentage error between the experimental results and the FE model predictions.

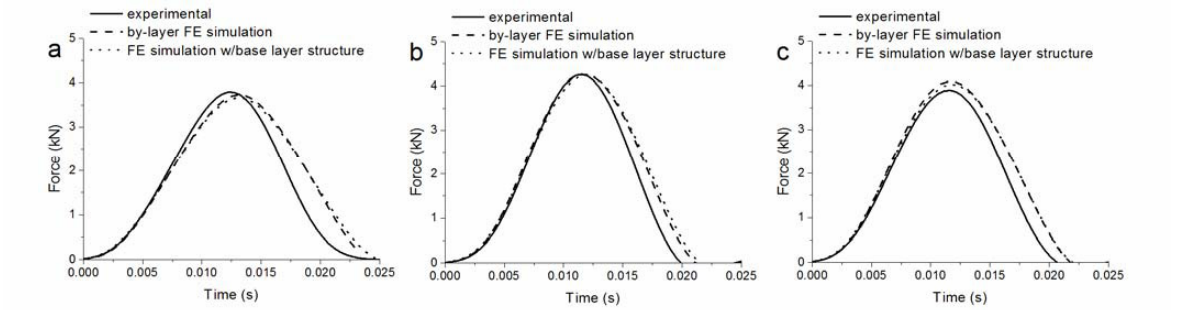

Fig. 4. Force exchanged between the test foot and materials (a) A, (b) D or (c) H during the impact time. Comparison between the experimental curves and the numerical model results, both processed with a Butterworth filter of the 9th order and cut-off frequency of 120 Hz.

Table 3. FR parameters exhibited by the considered tracks: comparison between the experimentally measured values and the FE predictions.

Materials	Experimental	Bi-layer FE simulation		FE simulation with base layer structure	
	FR (%)	FR (%)	Err (%)	FR (%)	Err (%)
A	39.1	40.0	2.5	41.2	5.3
D	31.5	31.4	0.5	31.7	0.5
H	37.5	35.5	5.2	34.2	8.6

The agreement between the newly developed 3D finite element model and the experimental force vs. time curves is very good for all three complete tracks studied; predicted values of FR are within a few percent points of the experimental ones. Predicted curves differ from the experimental data in the unloading part following the peak load: a possible explanation lies in the perfectly (although non-linear) elastic assumption made in the materials' constitutive modelling, which neglects any dissipative contribution arising from the inherent hysteresis of the rubbers used to produce the tracks, which has been verified by performing loading-unloading tests. This aspect had already been addressed in [8]; it doesn't significantly affect the determination of FR but it will have to be considered in further developments of the model to investigate energy restitution aspects, which are of paramount importance in defining the actual tracks' performance.

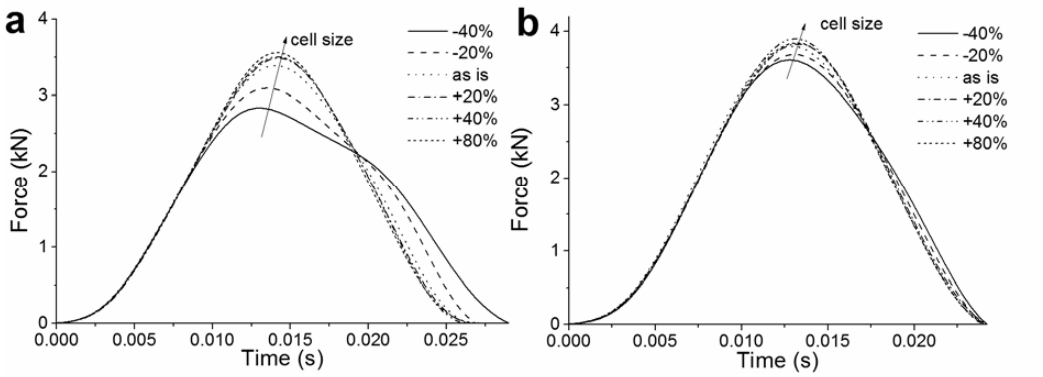

Fig. 5. Force exchanged between the test foot and modelled tracks derived from material (a) A or (b) H. Comparison between different factors of enlargement or reduction (to scale) of the base layer honeycomb structure. The curves were processed with a Butterworth filter of the 9th order and cut-off frequency of 120 Hz.

Finally, the size of the base layer honeycomb geometry proved to affect the overall impact behavior of the considered tracks. According to the results shown in Fig. 5, in fact, the FR parameter increases with the cell dimensions, exhibiting higher growing rates in the lower part of the investigated size range. A considerable effect on shape of the force-time curve was also observed in the case of track A during the unloading phase.

5. Conclusions

A three-dimensional finite element model was implemented, reproducing the impact behavior of running tracks as dependent on the pavement geometrical structure and material properties; experimental data were exploited to describe the compression behavior of such rubbers. The described model is able to predict in an accurate way both the force reduction parameter of a track and the overall time evolution of the force exchanged with the athlete's foot, especially in the loading phase. The predictions of the present model are in line with those obtained by an equivalent (2D) homogenized model. The improvement offered by the 3D implementation of the present model consists in taking into account, and correctly describing, the actual geometrical structure of the honeycomb base layers, which proved to have a considerable effect on the shock absorption ability of the overall track, thus making it a useful tool for the optimization of the running pavement performances, both in terms of material choice and of design of the honeycomb geometry. The next, obvious step will be the study of the effect of the geometrical parameters of the structure on the track response in the combined vertical and horizontal directions.

Acknowledgements

This work was supported by Fondazione Cariplo – project "Safer Helmets". The authors wish to thank MONDO SpA for supplying the materials; LP³ lab of Politecnico di Milano and Mr. Oscar Bressan for help in performing the experimental tests.

References

[1] EN 14808 Surfaces for sports areas—Determination of shock absorption, 2006.
[2] Benanti, M., Andena, L., Briatico-Vangosa, F., Pavan, A., 2013. Viscoelastic Behavior of athletics track surfaces in relation to their force reduction. Polymer Testing 32, 52-59.
[3] Andena, L., Briatico-Vangosa, F., Ciancio, A., Pavan, A., 2014. A finite element model for the prediction of Force Reduction of athletics tracks. Procedia Engineering 72, 847-852.
[4] Andena, L., Briatico-Vangosa, F., Cazzoni, E., Ciancio, A., Mariani, S., Pavan, A., 2015. Modeling of shock absorption in athletics track surfaces. Sports Engineering 18, 1-10.
[5] Baroud, G., Nigg, B.M., Stefanyshyn, D., 1999. Energy storage and return in sport surfaces. Sports Engineering 2, 173-180.
[6] Thomson, R.D., Birkbeck, A.E., Lucas, T.D., 2001. Hyperelastic modelling of nonlinear running surfaces. Sports Engineering 4, 215-224.
[7] Abaqus 6.13 User Manual. Dassault Systèmes, Providence, Rhode Island, 2013.
[8] Carré, M.J., James, D.M. & Haake, S.J., 2006. A hybrid method for assessing the performance of sports surfaces during ball impacts. Journal of Materials: Design and Applications 220, 31-39